



Development of a rapid heat cycle injection molding system using infrared radiation and convection heating and influence on morphology and mechanical properties

Ricardo Simoes^{1,2} · Cláudia Macedo¹ · Jorge Laranjeira³ · António M. Brito¹ · Carla L. Simões² · Luís Faria⁴

Received: 12 September 2023 / Accepted: 13 November 2023 / Published online: 24 November 2023
© The Author(s) 2023

Abstract

Conventional injection molding is widely used to produce plastic parts, mainly in the automotive industry, due to the high production ratios and quality of injection parts. Low mold temperatures are usually employed to decrease cycle molding time and final process costs; however, resulting surface defects include weld lines, sink marks, and warpage. Therefore, plastic parts are often subjected to secondary processes to reduce the surface defects. A dynamic mold heating and cooling control technology, rapid heat cycle molding (RHCM), was employed to optimize the injection molding process. The present study combined convection heating (pressurized water flow) and external infrared heating systems to investigate the effect of dynamic temperature control on the injection molding process. The infrared heating system was custom built to allow studying under controlled conditions the influence of several process parameters on the resulting morphology and mechanical properties. Results show significant gains from using the RHCM technology to optimize the conventional process, namely, at 100 °C no frozen layer is formed while simultaneously increasing the Young's modulus. Industrial companies struggling with defects resulting from the thermal changes during injection molding can thus consider RHCM as a mitigation strategy and use these results as a guide for tool design and implementation of the technique.

Keywords Injection molding · Dynamic temperature control · Infrared radiation (IR) · Heat cycle molding · Morphological properties · Mechanical characteristics

1 Introduction

The conventional plastic injection molding process is important for its ability to produce molded parts accurately

and quickly while allowing the manufacture of very complex geometries [1]. During the process, the melted polymer is injected into a mold cavity, packed, and cooled until it has solidified before being ejected to start another molding cycle [2]. Low mold temperatures (circa 50–60 °C)

Cláudia Macedo, Jorge Laranjeira, António M. Brito, Carla L. Simões, and Luís Faria contributed equally to this work.

✉ Ricardo Simoes
rsimoes@ipca.pt

Cláudia Macedo
id9230@alunos.uminho.pt

Jorge Laranjeira
jorge.laranjeira@moltdindustries.com

António M. Brito
amb@dep.uminho.pt

Carla L. Simões
csimoes@ipca.pt

Luís Faria
luis.faria@tecnico.ulisboa.pt

¹ Institute for Polymers and Composites (IPC), University of Minho, 4800-058 Guimarães, Portugal

² Polytechnic Institute of Cavado and Ave (IPCA), 4750-810 Barcelos, Portugal

³ Moldit – Mold Industry S.A., 3720-903 Oliveira de Azemeis, Portugal

⁴ Technical University of Lisbon (IST), Campus Alameda, 1049-001 Lisbon, Portugal

are used in conventional injection molding technology to reduce the cycle molding time. The rapid cooling of the plastic parts can cause surface defects such as weld lines, sink marks, or warpages [3]. The quality of the molded products remains a significant criterion [4]. When the defects are noticeably unacceptable, the plastic parts are often subjected to secondary processes or might have to be rejected entirely [5].

Different technologies have been developed to optimize the conventional injection molding processes. Rapid heat cycle molding (RHCM) is a non-conventional technology where the mold surfaces are heated and cooled repeatedly during the molding cycle to inject the material into a higher temperature mold than usual in traditional injection molding [6]. A heating system heats the mold surfaces to a high mold temperature, usually higher than the polymer's glass transition temperature; the high mold temperature is preserved during the filling and packing stage. Then, the mold surfaces are cooled by a cooling system, and the mold temperature decreases until it reaches the material ejection temperature, and, finally, the plastic part is ejected. In RHCM technology, the mold surface temperature is controlled dynamically and cyclically; therefore, the mold surfaces must be rapidly heated and cooled [7].

Different authors studied the defects of the plastic parts produced by the injection molding process. Bahur and Ibrahim and Yueh-Tzu et al. analyzed the warpage phenomenon in thin-walled parts [3, 8]. Yueh-Tzu et al. employed the "Moldflow" software to analyze the runner's balance on multi-cavities of thin-walled parts and simulate their warpage [8]. These authors also considered the influence of molding parameters on warpage, intending to optimize the process. Concerning an analogous and common problem of injection molding, other authors also used the "Moldflow" software, but in this case, to analyze the shrinkage of micro-injection molded plastic parts and determine the optimum processing parameters.

Several authors have already studied the advantages of RHCM on injection molded plastic parts, focusing on optimizing the process or eliminating defects. Keun and Sang-Ik applied the RHCM approach and identified the influence of defects on the plastic parts using numerical simulation [9]. Wang et al. also employed numerical thermal analysis to investigate the mold surface temperature response during heating and the temperature of the melt polymer during the cooling stage [10]. Lucchetta and Fiorotto also applied the RHCM technology and showed that it could reduce and eliminate the surface defects of the molded parts [11]. Sánchez et al. analyzed the mold cavity temperature provided by electric resistance heating and convection cooling in RHCM. They simulated the material's mechanical,

thermal, and rheological properties to study the effects of temperature on part defects [12].

Similarly, Wang et al. studied the effect of the heating/cooling system on the injection process but with steam heating and convection cooling [13]. Shia-Chung et al. measured the surface quality of the parts using a gas-assisted heating system in the injection molding process [14]. In summary, these different authors concluded that the RHCM process could improve the quality of the parts, namely, shrinkage and warpage (distortions of the intended shape of the molded part during the cooling stage) and weld marks, with particular impact on surface defects. In most cases, the authors have also determined the basic parameters of the injection molding process affected by RHCM.

Donggang and Byung and Poszwa et al. studied the RHCM's effects on basic parameters related to the filling stage, showing that the RHCM technology could lengthen the melt flow path [15, 16]. De Santis and Pantani developed and applied a temperature control system on micro-injection molding and studied the effect of mold temperature on the molten polymers' flow properties and the parts' morphology [17]. Keun and Sang-Ik and Liparoti et al. studied the injection molding parameters during the rapid heat cycle injection molding process [9, 18]. The authors found that the temperature of the mold can reduce the injection mold pressure. Wangging et al. (2022) defined and applied a temperature control system and studied the flow-induced molecular orientation of the molten polymers. The results showed that the molded plastic parts' microstructure depends on the mold's temperature.

The properties of the molded plastic parts are well known to be affected by the mold temperature. Since RHCM is essentially a non-conventional control of the mold temperature, it becomes important to realize how it will affect the material properties. The molding conditions' effect on morphology has been extensively reported, for example, ref. [19]. Feng et al. explored the mold surface temperature influence on the molded product's microstructure and measured the parts' macroscopic properties [20]. The authors observed that the molded parts' macroscopic properties (mechanical properties) depend on the mold temperature surface. Li et al. studied the molded part's microstructure and found that it depends on the crystallization parameters during the RHCM process [21]. Noguchi et al. demonstrated that heat treatments affect the molded parts' morphology and properties. The mechanical properties were affected by the microstructure of the parts. In turn, the mold temperature surface influences the microstructure, with the frozen layer (typically created upon contact of the front flow of the hot polymer melt with the colder mold surface) being highly sensitive to the mold surface temperature [22].

The mold surface temperature in RHCM must be controlled dynamically and cyclically, and there are different methods available in an industrial setting for efficient heating and cooling. Selection of the proper method is key to the success of the RHCM approach. Zhao et al. evaluated resistance heating methods to heat the mold surface [23]. Cheng-Long and Han-Xiong and also Xi-Ping et al. applied a resistance heating method (electrical heating system) for RHCM applications [24–26]. Alternatively, an induction heating system in the micro-injection molding process for rapid mold temperature variation was used by Shia-Chung et al. and also by Ming-Shyan and Ning-Sheng [27, 28]. Shia-Chung et al. measured the surface quality of the parts using an induction heating system in the injection molding process [29]. Keun and Sang-Ik applied a localized mold induction heating system for injection molding [9]. Dong-gang et al. and Shia-Chung et al. used a high-frequency proximity heating system for RHCM applications. At the same time, Pei-Chi and Sheng-Jye studied an infrared rapid surface heating system for injection molding [30–32]. Menghan et al. studied the effect of the convection heating (water-assisted heating) system using the RHCM approach in the injection molding process [33]. Ming-Chang et al., Guilong et al., and Liu et al. applied a steam heating system to heat the mold surface in the injection molding process [34–36]. Shayfull et al. reviewed the application of conformal cooling channels to reduce the rapid heating and cooling cycle time for the conventional injection molding process, which could eventually be employed to improve the RHCM approach [37]. Each of these was shown to have different features, but none of those studies directly compared two of the most promising techniques: infrared radiation and convection heating.

To complement the existing information on the practical application of the RHCM technology, the present paper combined infrared radiation heating and a convection (water

flow) temperature control system in optimizing injection molding RHCM using a case-study part.

2 Materials and methods

2.1 Mold

A new mold was produced for this study, with the aim of assessing the effect of the RHCM technology on the resulting part morphology and properties, for a standard dumbbell specimen. Figure 1 shows the complete 3D CAD model of the mold and the mold cavity of the standard tensile specimens.

The mold produces simultaneously two standard tensile specimens: the C-standard tensile specimens (center gate) and the E-standard tensile specimens (edge gate); see Fig. 2.

Figure 3 shows the mold plate's heating and cooling channels, which were used with the RHCM technology.

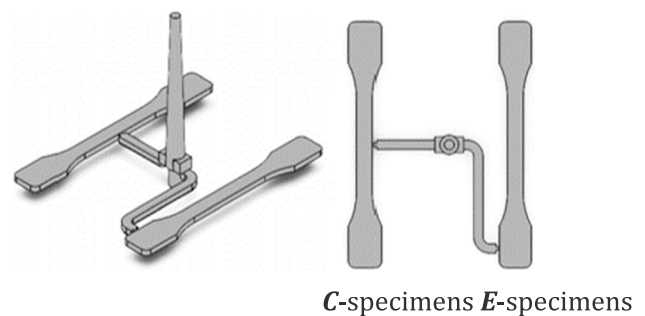


Fig. 2 Standard tensile specimens (3D CAD model) showing the “central” (C-specimens) and the “edge” (E-specimens) gate. The C- and E-standard tensile specimens’ dimensions are 70 mm (total length), 30 mm (length), 5 mm (width), and 2 mm (thickness)

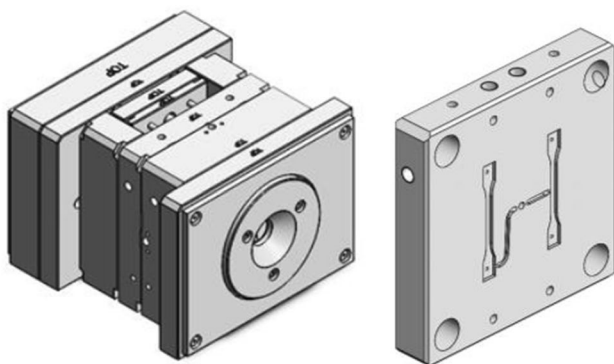


Fig. 1 The injection mold structure (3D CAD model) to produce the standard tensile specimens using RHCM technology

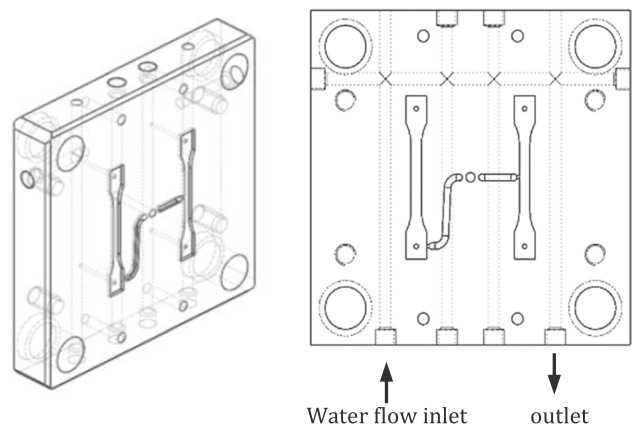


Fig. 3 The mold plate's heating and cooling channels create thermo-mechanical environments

2.2 Processing technology

The experimental setup comprises four components: an injection molding machine (BOY 22 A), the previously described mold, a thermoregulator (PIOVAN Thermovan TP), and a robot manipulator (PIKO pneumatic robot) to which an IR heating system is fixed. The infrared heating system was designed and manufactured for this specific study and allows heating the mold surfaces in a controlled manner. It is fixed to a pneumatic robot manipulator to allow moving the IR lamps into position to heat the mold surface when the mold is open and afterwards rapidly withdrawing to allow the mold to close. The mold temperature controller (thermoregulator) was used to dynamically control the temperature of the mold cavities by convection heating and

cooling the water flow at a controlled temperature inside the mold's heating and cooling channels. Figure 4 shows the injection molding machine and the IR heating system connected to the PIKO pneumatic robot.

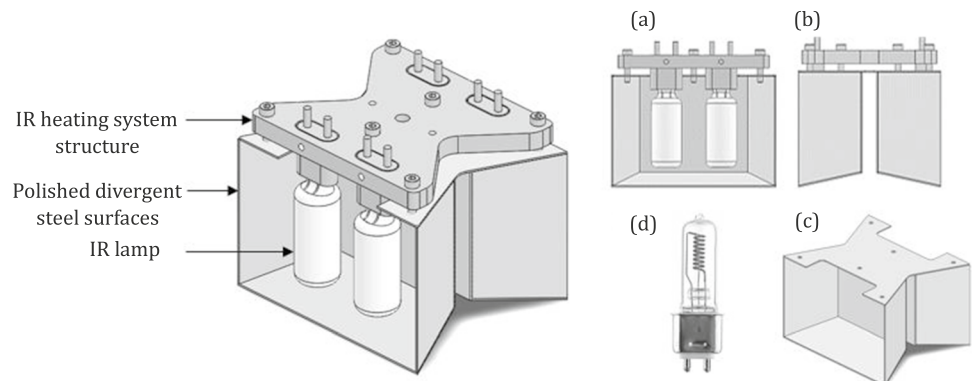
2.3 Infrared radiation heating method and system

In IR heating methods, the mold surface absorbs the infrared radiation emitted by the IR heating system. The IR heating system developed specifically for this work is illustrated in Figs. 5 and 6. It comprises two distinct elements: the lamp harness and the lamps. The highly polished divergent surfaces of the lamp harness direct the light emitted by the lamps to the mold surface. Up to four IR lamps can be used in the IR heating system.

Fig. 4 The BOY 22 A injection molding machine, the PIKO pneumatic robot, and the IR heating system (Laboratory of University of Minho)



Fig. 5 Infrared heating system illustration: (a) front view, (b) lateral view, (c) isometric view, and (d) IR lamp (OSRAM)



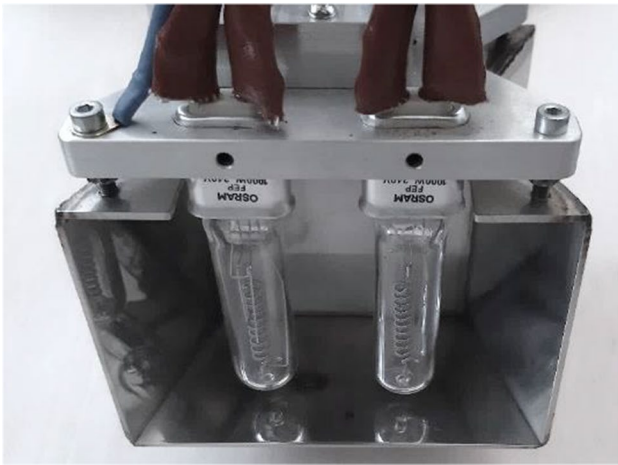


Fig. 6 Infrared heating system: IR lamp, lamp structure, and electrical system of the heating system

3 Influence of the IR system on the heating efficiency

3.1 Experimental plan

A study was conducted to evaluate the efficiency of the heating system. The study was designed to help in the subsequent selection of the optimal setup to study the influence of the molding parameters on the material properties and morphology.

The first test evaluates the influence of the distance between the IR lamps and the mold surface. The test evaluates the temperature in position P2 of the mold surface (a center position at equal distance to the 2 tensile specimen cavities), when the IR lamps are at a distance from the mold surface of 5, 10, 15, 20, 25, and 30 mm (distances D1, D2, D3, D4, D5, and D6, respectively). The schematic

Fig. 7 Position P2 of thermometer and location of the IR heating system lamps: the IR heating system aligned centered with the mold cavity of the C- and E-standard specimens

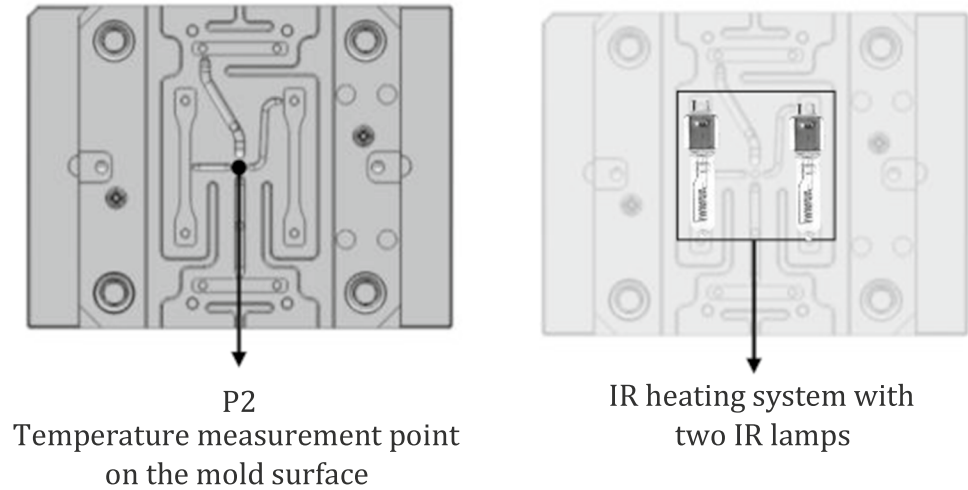


Fig. 8 Position of the P1, P2, and P3 and position of the IR heating system: the IR heating system aligned with the mold cavity of the E-standard specimens

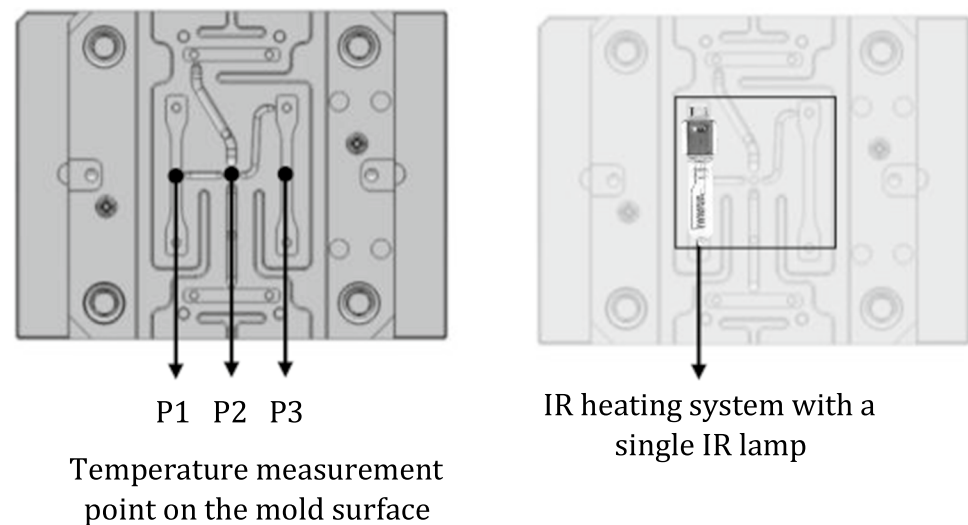


Table 1 Experimental plan for the IR lamps alignment with the mold cavities (values in mm)

Distance of the IR system from mold surface (mm)	Distance of the thermometer from the center line of the lamp of the heating system (mm)
5 mm from mold surface (D1)	P1 = 0 mm
	P2 = 50 mm
	P3 = 100 mm
30 mm from mold surface (D6)	P1 = 0 mm
	P2 = 50 mm
	P3 = 100 mm

representation of the position of the thermometer at the P2 location for the distance tests is shown in Fig. 7.

The second test assesses the influence of the alignment of the lamp with the mold cavity. The temperature was measured on the positions P1, P2, and P3 of the IR system at a mold surface distance of 5 mm (D1) and 30 mm (D6), to determine the temperature distribution. The schematic representation of the thermometer positions (P1, P2, and P3) is shown in Fig. 8, and the respective experimental plan is described in Table 1.

3.2 Experimental procedure

The thermoregulator is triggered to heat the mold surfaces until the mold temperature equals 40 °C; then, the equipment is turned off, and the IR heating system is activated, moving into the proper position (at the pre-determined distance from the mold surface). After a set time, the heating system is switched off, and the temperature of the mold surfaces is measured on positions P1

through P3 (or only P2 depending on the study). Finally, the equipment with a pressurized water system is activated to promote the cooling of the mold surfaces. The procedure is repeated at different distances (distances D1 through D6).

3.3 Heating efficiency results

Figure 9 describes the evolution of the heating rate for the various distances from the IR lamps to the molding surface (D1 through D6). As expected, the heating rate depends significantly on the distance from the IR lamps to the mold surface. For distance D1 (5 mm from the mold surface), the heating rate is equal to 30.9 °C/min, while for distance D6 (30 mm from the mold surface), the heating rate decreases by 42.7% to 17.7 °C/min.

Figure 10 presents the values of the heating rate of the IR heating system at different mold surface positions (P1, P2, and P3), both at the smallest and largest distance of the IR lamps to the mold surface (distances D1

Fig. 9 Heating rate variation with the distance from the IR lamps to the mold surface (from D1 = 5 mm to D6 = 30 mm)

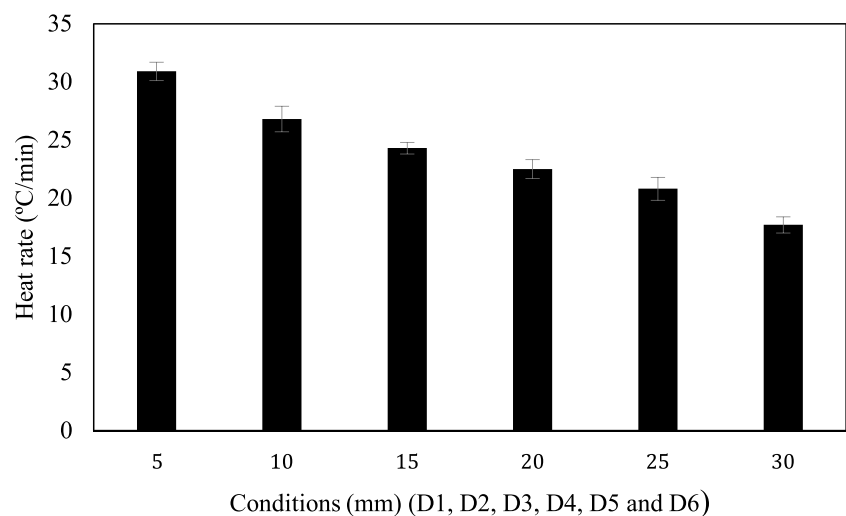
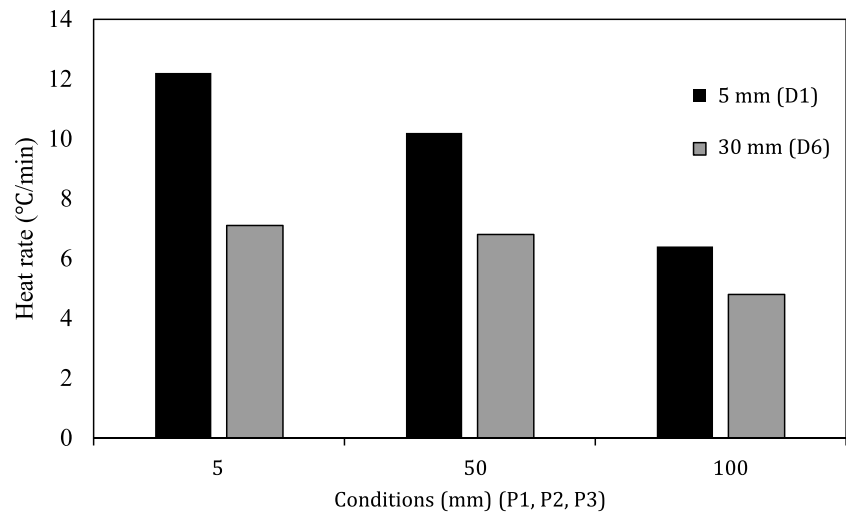


Fig. 10 Heating rate variation with the position of the thermometer from the center line of the lamp of the heating system (P1, P2, and P3)



and D6, respectively). The heating rate of the IR heating system is considerably higher in distance D1 than distance D6, regardless of the position of the thermometer from the centerline of the lamp of the heating system.

The results indicate a significant temperature gradient on the mold surface promoted by the asymmetric configuration of the IR heating system; that is, the heating rate is higher at position P1 (directly aligned with the IR lamp) and lower at position P3 (the cavity away from the IR lamp). At the smallest distance between the IR lamps and the mold surface (D1 of 5 mm), the heating rate decreases 47.5% from P1 to P3. Even at the highest distance (D6 of 30 mm), where the heating rate of P1 is already much lower (circa 58% lower) than when the distance is 5 mm, the heating rate of the IR heating system still decreases 32.4% from P1 to P3. All individual measurements of the heating rate are provided in Appendix Tables 3 and 4.

In terms of temperature uniformity, when the mold was at the temperature of circa 40 °C, the range of temperatures at the 3 measured points was at most 1.5 °C (on average 0.5 °C), while at a temperature of 70 °C, the range was at most 2 °C (on average 1.5 °C).

Table 2 The three (conditions A, B, and C) thermomechanical environments during the molding cycle. In condition C, the mold temperature is dynamically controlled

Condition	Temperature of the mold surfaces (°C) filling and packing stage of the cycle molding	Temperature of the mold surfaces (°C) cooling stage of the cycle molding
A	40	40
B	70	70
C	100	70

4 Influence of the molding parameters on the materials properties and morphology

4.1 Experimental plan

The influence of the RHCM technology molding parameters, namely, the temperature of the mold surfaces at different stages of the injection molding process, on the properties and morphology of the final part, an experimental plan was devised with three conditions, as shown in Table 2. Other injection molding parameters, namely, the injection temperature of the testing material adopted was 230 °C (polypropylene SABIC 579 P) and injection speed was 30 mm/s, injection pressure was 100 bar, and the holding pressure was 40 bar, were kept for all conditions.

4.2 Experimental procedure

At the beginning of the molding cycle, the pressurized water system equipment is activated to heat the mold surfaces until the mold temperature of 40 °C (condition A) or 70 °C (conditions B and C). In condition C, after the mold surface is at 70 °C, the pressurized water system equipment is turned off and the IR heating system is activated at the optimal position (which was determined from the heating efficiency analyses), until the mold temperature reaches 100 °C. Then, the IR heating system is switched off (and moved away from the mold), the mold closes, and the specimens are molded. After the packing stage, the pressurized water system equipment is again activated to cool the mold until the material ejection temperature of 70 °C. Thus, in condition A, the pressurized water system is always kept at 40 °C, while in conditions B and C it is always kept at 70 °C.

4.3 Characterization of the molded parts

The employed RHCP approach is expected to have an influence on both the mechanical properties and the morphological features of the molded parts. As such, a characterization plan was prepared to evaluate the influence of the RHCM technology parameters, namely, on the Young's modulus (as the stiffness is a common engineering requirement in material selection) and on the frozen layer fraction (which in turn could affect the stiffness of the material).

The Young's modulus was extracted from tensile tests results, comparing the performance of both C- and E-standard tensile specimens, under the following conditions: INSTRON 5969 universal tensile testing machine composed of non-contacting video extensometers; test speed: 50 mm/min; grips distance: 50 mm; Standard ASTM D 638.

Fig. 11 The Young's modulus profile of the standard tensile specimens with the mold surface temperature

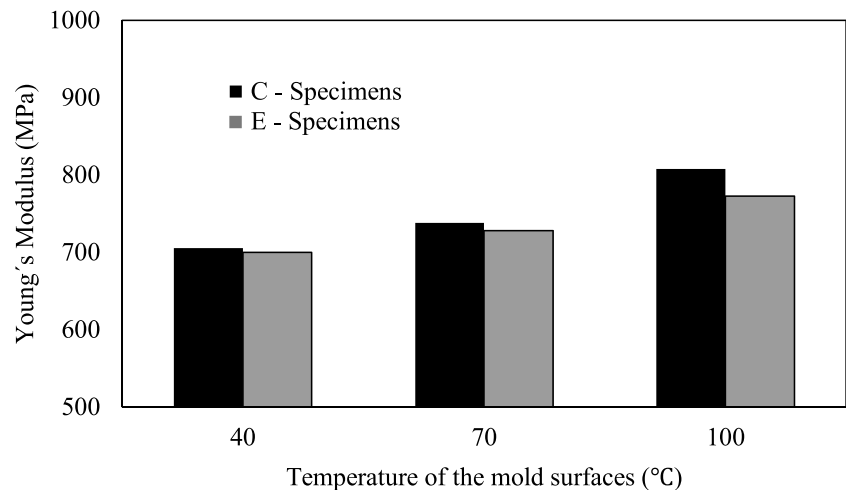
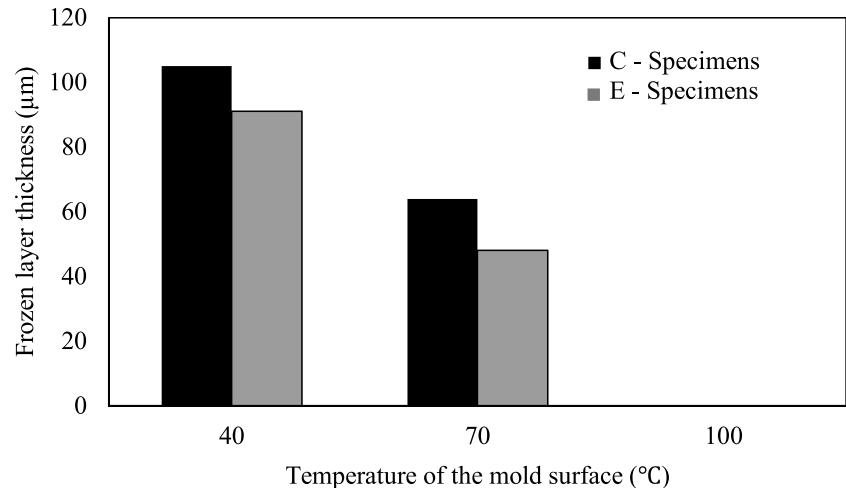


Fig. 12 Frozen layer thickness evolution for conditions A, B, and C of the C- and E-standard tensile specimens



The frozen layer fraction was measured by optical microscopy, specifically using polarized light microscopy, and again comparing the C- and E-standard tensile specimens, under the following experimental conditions: (1) sample preparation on a microtome; (2) microscopic analysis on an OLYMPUS BH-2 transmission optical microscope.

All experimental tests were performed at the Polymer Engineering Department of the University of Minho, Portugal. The respective results are shown and discussed in Sections 4.4 and 4.5.

4.4 Mechanical properties results and analysis

Figure 11 describes the dependance of the Young's modulus on the mold surface temperature for the C- and E-standard tensile specimens. All measurements are also provided in Appendix Table 5.

The mold surface temperature has a significant influence on the Young's modulus of the plastic parts, with the C-standard tensile specimens exhibiting slightly higher values than those of the E-standard tensile specimens for the mold temperatures range under evaluation. Namely, the Young's modulus increases from 705.4 MPa at 40 °C to 807.9 MPa at 100 °C (a 14.5% increase) for the C-standard tensile specimens, and it increases from 700 MPa at 40 °C to 772.4 MPa at 100 °C (a 10.3% increase) for the E-standard tensile specimens. Thus, irrespective of the gate location, the Young's modulus is higher with the RHCM approach, increasing with the mold surface temperature.

4.5 Frozen layer thickness results and analysis

The frozen layer, typically created upon contact of the front flow of the hot polymer melt with the colder mold surface, is one of the parameters expected to be most dependent on the mold surface temperature, and also has

a high influence on tribological and esthetic properties, namely, gloss (and also transparency for some polymers). The frozen layer also affects the molding quality, in terms of shrinkage, warpage, and in some cases is responsible for residual stresses, all of which are expected to be improved using the RHCM technology.

Figure 12 shows the influence of the mold surface temperature on the frozen layer thickness for the C- and E-standard tensile specimens. The increase of the mold temperature from 40 to 70 °C decreases the frozen layer thickness by 39.0% in the case of C-standard tensile specimens and by 47.3% in the case of E-standard tensile specimens. When the mold temperature is increased to 100 °C, no frozen layer is observed, regardless of the location of the injection gate. Thus, using RHCM to heat the molding surface to 100 °C would, in this case, entirely prevent the formation of a frozen layer, with an expected positive effect on the previously mentioned defects and issues. Obviously, these results pertain to a simple standard tensile test geometry, and a more

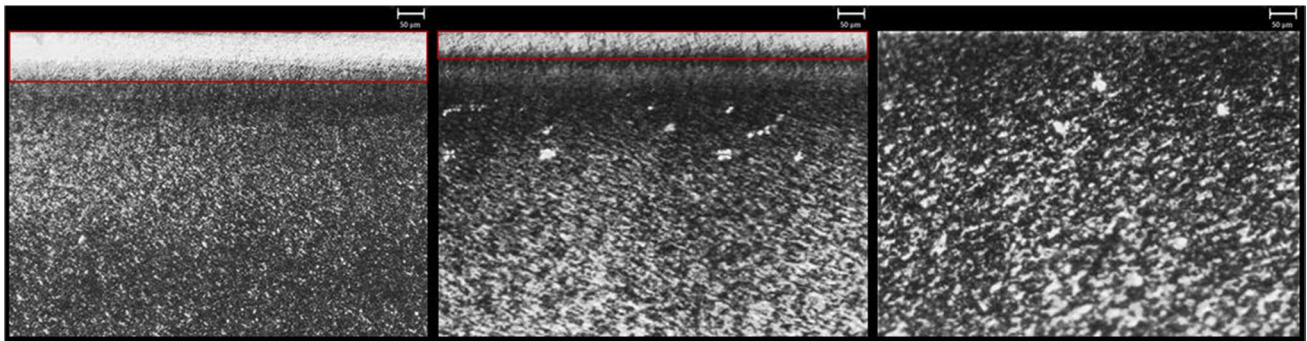


Fig. 13 Frozen layer thickness of the C-standard tensile specimens at 40 °C (left), 70 °C (center), and 100 °C (right) mold surface temperature (resolution: 20×1.67 ; a scale of 50 μm is shown embedded in the micrographs)

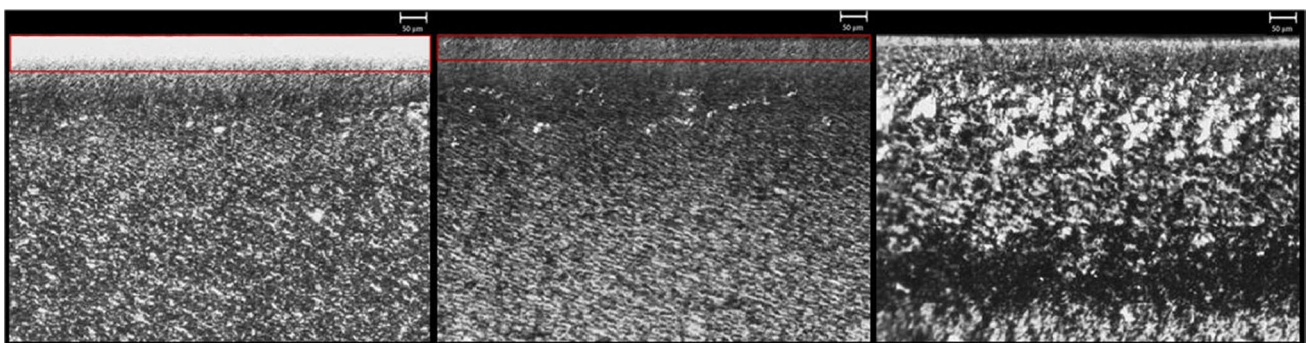


Fig. 14 Frozen layer thickness of the E-standard tensile specimens at 40 °C (left), 70 °C (center), and 100 °C (right) mold surface temperature (resolution: 20×1.67 ; a scale of 50 μm is shown embedded in the micrographs)

complex part will behave differently, but in any case, an optimum mold surface temperature can be identified if a frozen layer is to be avoided.

Note that while the decrease of the frozen layer could have been expected to reduce the Young's modulus, this did not happen, as shown in the previous section. This is a very positive outcome and is related with the specific orientation at which the frozen layer is formed and its morphology, and other geometries might behave differently which implies the need to perform similar validation and optimization tests for each specific geometry to be injection molded using RHCM. Measurements of the frozen layer thickness were made using a transmission optical microscope (OLYMPUS BH-2), and the obtained micrographs transferred to the microscope's digital imaging software for analysis. The thickness of the layer is obtained directly from the imaging software by drawing the region which corresponds to the frozen layer. Figures 13 and 14 show the morphology of the specimens between 40 and 100 °C, respectively, for the C-standard and E-standard cases. It should also be noted that no discernible shrinkage or warpage occurred, which can be attributed to the high mold surface temperature contributing to a more uniform cooling and the lack of residual stresses.

5 Conclusions

An IR heating system was developed and added to a conventional injection molding process to study the RHCM approach, namely, the influence of the key RHCM parameter (the mold surface temperature) on important part features (namely, the Young's modulus and the frozen layer fraction). Preliminary tests were conducted to optimize the experimental setup, namely, the distance between the IR lamps and the mold surface, and the location of the lamps with respect to the molding cavities.

As expected, a temperature gradient appears on the mold surface, showing the importance of aligning the IR lamps with the cavity, and the heating rate was found to be highly dependent on the distance from the IR lamps to the surface, thus affecting the system performance (namely, the cycle time, with significant impact on production volumes, etc.).

With the use of the RHCM approach, a significant increase of the Young's modulus was observed of 14.5% in the case of C-standard tensile specimens and 10.4% in the case of E-standard tensile specimens, when the mold temperature was increased from 40 to 100 °C. Additionally, at a mold surface temperature of 100 °C, the frozen layer disappeared entirely, and even at 70 °C, it was 39.0 to 47.3% smaller than the frozen layer thickness at 40 °C (respectively for the C-standard and E-standard tensile specimens). Thus, RHCM at 100 °C surface temperature prevented the formation of a frozen layer while simultaneously slightly increasing the Young's modulus. The parts exhibited no discernible shrinkage or warpage, due to the lack of residual stresses (although obviously these effects vary significantly for different geometries).

It was shown that a simple setup that couples the injection machine's thermoregulator (to reach a temperature of 40 °C), to a standard robot manipulator for positioning the IR lamps harness (and reach the desired mold temperature), can be an effective means of implementing RHCM. The obtained results highlight the potential of RHCM technology in injection molding, namely, as a strategy to mitigate or solve problems in challenging parts, either in terms of molding defects (e.g., warpage) or surface quality (e.g., gloss). Thus, these results have high industrial importance, given the very limited literature available on practical application of RHCM. The specific influence of RHCM on warpage and gloss will be studied in future work.

Appendix Heating rate of the IR system results (test of the heating efficiency)

Table 3 Heating rate of the IR system at conditions D1, D2, D3, D4, D5, and D6

Distance of the IR system from mold surface (mm)	Heat rate (°C/min)
5	30.9 ± 0.8
10	26.8 ± 1.1
15	24.3 ± 0.5
20	22.5 ± 0.8
25	20.8 ± 1.0
30	17.7 ± 0.7

Table 4 Heating rate of the IR system at positions P1, P2, and P3, for conditions D1 (5 mm) and D6 (30 mm)

Distance of the IR system from mold surface (mm)	Distance of the thermometer from the center line of the heating system lamp (mm)	Heat rate (°C/min)
5	0	12.2 ± 1.0
5	50	10.2 ± 0.8
5	100	6.4 ± 0.4
30	0	7.1 ± 0.8
30	50	6.8 ± 0.5
30	100	4.8 ± 0.2

Table 5 Young's modulus of the C- and E-standard tensile specimens at conditions A, B, and C

Condition	Mold surfaces temperature (°C)	C-standard specimen Young's modulus (MPa)	E-standard specimen Young's modulus (MPa)
A	40	705.4 ± 1.0	699.9 ± 1.6
B	70	737.9 ± 3.7	728.0 ± 5.2
C	100	807.9 ± 5.3	772.4 ± 5.7

Funding Open access funding provided by FCT/IFCCN (b-on). The work was funded by FEDER funds through the COMPETE 2020 program (project SAM, POCI-01–0247-FEDER-017620) and FCT—Portuguese Foundation for Science and Technology, through projects UIDB/05256/2020 and UIDP/05256/2020. The funding agencies had no influence on the content of the work or the preparation of this manuscript.

Declarations

Competing interests The authors declare no competing interests.

Open Access This article is licensed under a Creative Commons Attribution 4.0 International License, which permits use, sharing, adaptation, distribution and reproduction in any medium or format, as long as you give appropriate credit to the original author(s) and the source, provide a link to the Creative Commons licence, and indicate if changes were made. The images or other third party material in this article are included in the article's Creative Commons licence, unless indicated otherwise in a credit line to the material. If material is not included in the article's Creative Commons licence and your intended use is not permitted by statutory regulation or exceeds the permitted use, you will need to obtain permission directly from the copyright holder. To view a copy of this licence, visit <http://creativecommons.org/licenses/by/4.0/>.

References

- Huamin Z (2013) Computer modeling for injection molding: simulation, optimization, and control. Wiley, Hoboken
- Malloy RA (2010) Plastic part design for injection molding: an introduction, Cincinnati, Ohio, USA
- Bahur O, Ibrahim S (2009) Warpage and structural analysis of thin shell plastic in the plastic injection molding. *Mater Des* 30:367–375. <https://doi.org/10.1016/j.matdes.2008.04.053>
- Osswald TA, Turg LS, Gramann PJ (2002) Injection molding handbook. Munich, Germany
- Wang G, Zhao G, Li H, Yanjin G (2009) Research on a new variotherm injection molding technology and its application. *Polym-Plast Technol Eng* 48:671–681. <https://doi.org/10.1080/03602550902824549>
- Donggang Y, Shia-Chung C, Byung K (2009) Rapid thermal cycling of injection molds: an overview on technical approaches and applications. *Adv Polym Technol* 27:233–255. <https://doi.org/10.1002/adv.20136>
- Chris D, Rickey D, Wan LG (2004) Temperature control of injection molding. Part I: modeling and identification. *Polym Eng Sci* 44:2304–2317. <https://doi.org/10.1002/pen.20258>
- Yueh-Tzu H, Chiung-Fang H, Bou-Yue P, Chun-Wei C, Hsing-Chung C, Yi L, Yung-Kang S, Hao W (2020) Experimental and numerical study determining the warpage phenomenon of thin-wall injection molding. *Adv Polym Technol* 20:2914801
- Keun P, Sang-Ik L (2010) Localized mold heating with the aid of selective induction for injection molding of high aspect ratio micro-features. *J Micromech Microeng* 20:035002
- Wang G, Zhao G, Li H, Guan Y (2010) Research of thermal response simulation and mold structure optimization for rapid heat cycle molding processes, respectively, with steam heating and electric heating. *Mater Des* 31:382–395
- Lucchetta G, Fiorotto M (2013) Influence of rapid mold temperature variation on surface topography replication and appearance of injection-molded parts. *J Mech Eng* 11:539–542. <https://doi.org/10.1016/j.cirp.2012.03.091>
- Sánchez R, Martínez A, Mercado D, Carbonel A, Aisa J (2021) Rapid heating injection moulding: an experimental surface temperature study. *Polym Testing* 93:106928. <https://doi.org/10.1016/j.polymertesting.2020.106928>
- Wang G, Zhao G, Li H, Guan Y (2010) Analysis of thermal cycling efficiency and optimal design of heating/cooling systems for rapid heat cycle injection molding process. *Mater Des* 31:3426–3441
- Shia-Chung C, Pham MS, Jen-An C (2011) Gas-assisted mold temperature control for improving the quality of injection molded parts with fiber additives. *Int Commun Heat Mass Transfer* 38:304–312
- Donggang Y, Byung K (2007) Increasing flow length in thin wall injection molding using a rapidly heated mold. *Polym-Plast Technol Eng* 41:819–832
- Poszwa P, Muszynski P, Mrozek K (2020) Numerical study on the influence of RHCM on the basic parameters of filling cavity. *J Manuf Sci Technol* 30:94–104. <https://doi.org/10.1016/j.cirpj.2020.04.007>
- De Santis F, Pantani R (2016) Development of a rapid surface temperature variation system and application to micro-injection molding. *J Mater Process Technol* 237:1–11. <https://doi.org/10.1016/j.jmatprotec.2016.05.023>
- Liparoti S, Sorrentino A, Titomanlio G (2019) Temperature and pressure evolution in fast heat cycle injection molding. *Mater Manuf Process* 34:422–430. <https://doi.org/10.1080/10426914.2018.1512120>
- Viana J, Simoes R, Mano JF, Oliveira MJ, Denchev ZZ, Brostow W, Cunha AM (2010) Thermomechanical processing environment and morphology development of a thermotropic polymer liquid crystal. *J Appl Polym Sci* 115:2991
- Feng L, Taidong L, Fuyu X, Jiquan L, Shaofei J (2020) Microstructure, tensile property, and surface quality of glass fiber reinforced polypropylene parts molded by rapid heat cycle molding. *Adv Polym Technol* 20:3161068
- Li J, Li T, Yang S, Jiang S, Turg L-S (2018) Modeling and characterization of crystallization during rapid heat cycle molding. *Polym Testing* 71:182–191. <https://doi.org/10.1016/j.polymertesting.2018.09.004>
- Noguchi T, Niihara K, Kawamoto K, Fukushi M, Jinnai H, Nakajima K, Endo M (2021) Preparation of high-performance carbon nanotube/polyamide composite materials by elastic high-shear kneading and improvement of properties by induction heating treatment. *J Appl Polym Sci* 138:e50512. <https://doi.org/10.1002/app.50512>
- Zhao G, Wang G, Guan Y, Li H (2011) Research, and application of a new rapid heat cycle molding with electric heating and coolant cooling to improve the surface quality. *Polym Adv Technol* 22:476–487
- Cheng-Long X, Han-Xiong H (2014) Development of a rapid thermal cycling molding with electric heating and water impingement cooling for injection molding applications. *Appl Therm Eng* 73:712–722
- Cheng-Long X, Han-Xiong H (2013) Multiobjective optimization design of heating system in electric heating rapid thermal cycling mold for yielding high gloss parts. *J Appl Polym Sci* 131:39976. <https://doi.org/10.1002/app.39976>
- Xi-Ping L, Ning-Ning G, Yan-Jin G, Guang-Ming C (2011) Thermal and stress analysis of rapid electric heating injection mold. *Appl Therm Eng* 31:3989–3995
- Shia-Chung C, Wen-Ren J, Yaw-Jen C, Jen-An C, Jin-Chuan C (2006) Rapid mold temperature variation for assisting the micro injection of high aspect ratio micro-feature parts using induction heating technology. *J Micromech Microeng* 16:1783–1791

28. Ming-Shyan H, Ning-Sheng T (2009) Experimental rapid surface heating by induction for micro injection molding of light guided plates. *J Appl Polym Sci* 113:1345–1354
29. Shia-Chung C, Yu-Wan L, Rean-Der C, Hai-Mei L (2009) Variable mold temperature to improve surface quality of microcellular injection molded parts using induction heating technology. *Adv Polym Technol* 27:224–232
30. Donggang Y, Thomas KE, Byung K (2006) High frequency proximity heating for injection molding applications. *Polym Eng Sci* 46:938–945
31. Shia-Chung C, Pham MS, Jen-An C, Sung-Wei H, Chung-Huan H (2012) Mold temperature control using high-frequency proximity effect induced heating. *Int Commun Heat Mass Transfer* 39:216–223
32. Pei-Chi C, Sheng-Jye H (2006) Experimental investigation of infrared rapid surface heating for injection molding. *J Appl Polym Sci* 102:3704–3713. <https://doi.org/10.1002/app.24515>
33. Menghan W, Wenhao W, Jie Z, Zhong D, Xinru Z, Xuaobing Y (2013) Optimal design of medium channels for water-assisted rapid thermal cycle mold using multi-objective evolutionary algorithm and multi-attribute decision-making method. *Int J Adv Manuf Technol* 68:2407–2417. <https://doi.org/10.1007/s00170-013-4868-2>
34. Ming-Chang J, Shia-Chung C, Pham MS, Jen-An C, Chia-Shen C (2010) Rapid mold temperature control in injection molding by using steam heating. *Int Commun Heat Mass Transfer* 37:1295–1304
35. Guilong W, Guoqun Z, Huiping L, Yanjin G (2010) Analysis of thermal cycling efficiency and optimal design of heating/cooling systems for rapid heat cycle injection molding process. *Mater Des* 31:3426–3441
36. Liu J, Zhao G, Wang G, Guan Y (2011) Fully coupled transient heat transfer and melt filling simulation in rapid heat cycle molding with steam heating. *Polym-Plast Technol Eng* 50:423–437. <https://doi.org/10.1080/03602559.2011>
37. Shayfull Z, Sharif S, Zain AM, Ghazali MF, Mohd Saad R (2014) Potential of conformal cooling channels in rapid heat cycle molding: a review. *Adv Polym Technol* 33:21381. <https://doi.org/10.1002/adv.21381>

Publisher's Note Springer Nature remains neutral with regard to jurisdictional claims in published maps and institutional affiliations.